J Mater Sci (2007) 42:6762–6768
DOI 10.1007/s10853-006-1461-1

Systematic study on the influence of growth parameters on island density exponent, size distribution and scaling behaviour

Shankar Prasad Shrestha · Chong-Yun Park

Received: 4 April 2006 / Accepted: 15 December 2006 / Published online: 27 April 2007

Abstract We present the Monte Carlo simulation of submonolayer film growth during molecular beam epitaxy (MBE) at low temperature. We have made systematic study to see how the parameters diffusion to flux ratio (D/F), diffusional anisotropy (DA) and sticking anisotropy influences on island density exponent (χ), size distribution and scaling behaviour. We have found that, as diffusional anisotropy changes from DA = 1 to DA = ∞, the density exponent changes from $\chi = 0.34 \pm 0.01$ to 0.28 ± 0.01 for isotropic sticking case but when sticking is anisotropic the density exponent changes from $\chi = 0.31 \pm 0.01$ to 0.24 ± 0.01. The influence produced by DA on island size distribution is observed to depend on D/F ratio and sticking anisotropy. Depending on DA values and D/F ratio, the size distribution is also observed to be insensitive to the change in diffusional anisotropy. We also study the influence of diffusional anisotropy on scaling function for two sticking anisotropy condition. The scaling behaviour of island size distribution is observed to be not affected by all diffusional anisotropy as well as sticking anisotropy condition.

S. P. Shrestha (✉)
Department of Physics, Tribhuvan University, Patan Multiple Campus, Patan Dhoka, Lalitpur, Nepal
e-mail: shankarpds@yahoo.com

C.-Y. Park
Department of Physics, Sung Kyun Kwan University, Suwon 440-746, South Korea

Introduction

Recently, the problem of submonolayer epitaxial growth has received considerable interest [1–14] due to its immense practical importance. It is because the multi layer surface morphology is basically dependent on the surface morphology and size distribution in submonolayer [8]. The fundamental process involved in epitixial growth such as molecular beam epitaxy (MBE) are deposition of adatoms with flux F on the substrate and diffusion of adatoms on substrate resulting nucleation, aggregation and coalescence of islands. These process leads to the formation of distribution of islands of various sizes. Understanding how the island density, island size distribution is affected by the parameters such as D/F ratio, diffusional anisotropy as well as sticking anisotropy is very important in epitixial growth of thin film. From the experimental study of submonolayer growth one can also calculate the important quantity such as diffusion constant $D = Do \exp(-Ea/KT)$ and the activation energy Ea of the surface diffusion. To calculate these quantities experimentally, one generally measures the scaling of island density N as a function of temperature and deposition flux in precoalescence regime. Using the scaling relation $N \sim (D/F)^{-\chi}$ the scaling exponent χ is determined by measuring the variation of N as a function of deposition flux at fixed temperature. From the known value of the exponent χ and using experimental temperature dependence of total island density, the activation energy Ea and also the prefactor of diffusion constant Do is determined. Thus, knowledge of scaling behaviour of the island density and size distribution is very important to determine the important physical quantity of epitixial growth. Using such technique as well as with the aid of Monte Carlo simulation, several groups have measured the activation energy as well as prefactor of diffusion constant in various system [4, 5, 15–20].

The scaling relation for total island number density was studied by several groups using different models. Using model with point island [13] dendritic islands [14] as well as compact islands [15], the density exponent $\chi = 1/3$ are reported for isotropic diffusion case. For anisotropic diffusion case using point island model [13, 15], the value of χ was found to be between 1/3 and 1/4 depending on degree of anisotropy, where as in model with compact island [15], $\chi \sim 1/3$ was observed. Using model in which the adatoms aggregate as dimerized chains [5], the exponent χ were found to be 1/3 and 1/4 for DA = 1 and DA = 1,000, respectively. Using similar model, the other group [21] found the exponent to remain fixed $\chi = 1/3$ in these range of diffusional anisotropy. These groups have analyzed average island length instead of island density. Further, the later groups also have studied the scaling of dimer chain size distribution with D/F ratio. Using a variant of model deposition diffusion and aggregation of particle forming 1d islands in square lattice [22], the island density exponent χ were found to vary from 1/3 to 1/4 as DA change from 1 to a very high value (DA $< \infty$). In spite of great deal of work systematic study of the dependence of size distribution and scaling behaviour on each deposition parameters is still lacking to our knowledge. In this work, we made systematic study to observe the influence of diffusional anisotropy, D/F ratio at two different sticking conditions on island density exponent, size distribution and scaling behaviour. We show how DA shows its influence on presence of other deposition parameter.

Model and simulation

Our simulation and model used closely resembles the Monte Carlo solid-on-solid simulation model used by Labella [20]. Using this model, they have successfully generated the similar island morphologies obtained by STM at different temperature. By combined study of simulated morphologies and temperature dependent STM morphologies, they have successfully determined the diffusion parameter for Ga on GaAs (001)-2 × 4 surfaces.

In our model, the monomers encounters the following process before the final island morphology is formed (a) Deposition and diffusion: Monomers are deposited randomly at constant flux (F) of 1/600 mL per sec, on a square lattice of size 600 × 600. The deposited monomers are allowed to diffuse to nearest neighbour (NN) sites by random jump. Each jumping adatom is selected at random among the existing monomers, which are not sticked to island in the substrate. Similarly, NN site for jump of adatom is also selected randomly. The jump at the selected site is allowed only if it is not occupied by another atom. In order to take account of diffusional anisotropy, any attempt to jump to NN site in x direction or y direction is made successful according to the preset value of the diffusional anisotropy parameter (DA). The parameter DA is dimensionless parameter which is simply a diffusional probability ratio DY/DX, where DY (DX) is the diffusion probability of monomer along Y and X direction in unit of jump per sec. and D = DY + DX. When the depositing monomer encounters the top of existing monomer or island, it is allowed to jump in one of the NN site chosen at random. If the NN site is also the top of an island, then for simplicity another site of deposition is chosen. For low coverage, this will not affect the resulting morphology because probability of such event is quite low. The deposition is stopped when final coverage of 0.07 mL is reached. In order to avoid edge effect, periodic boundary condition were applied in both X and Y direction. (b) Nucleation and aggregation: When the deposited monomer or diffusing monomer encounters another monomer in nearest neighbour site, a stable two adatoms island is allowed to nucleate with certain probability depending on the initial preset sticking anisotropy parameter (SA). As in the diffusional anisotropy case, the parameter SA is simply a sticking probability ratio (SY/SX), where SY (SX) is the sticking probability along Y and X direction of the substrate. Here, the sticking probability simply means the ratio of the total number of successful sticking to the stable island to the total number of attempts. Since we do not allow island dissociation, our simulation is basically for low temperature MBE island growth. When the deposited monomer or diffusing monomer encounters an existing island, it is allowed to stick in similar way as in the case of monomer. When it sticks to its nearest neighbour site, the number of atoms in the island is increased by 1. If the adatom does not stick to the NN site then it is treated as monomer and allowed for further diffusion. The simulation codes were developed by using Fortran 90 developer. In order to study the influence of each parameter DA, SA and D/F on island morphology we have monitored island morphology for various D/F ratios from 600 to $6 * 10^6$. These whole simulations are repeated for two extreme sticking case SA = 1(isotropic sticking case) and SA = 0 (anisotropic sticking case). In isotropic sticking case, with unit sticking probability in both Y (the direction of fast diffusion) and X (perpendicular to the direction of fast diffusion), the value of sticking anisotropy parameter SA = SY/SX becomes one. In this case, the monomer aggregates as it touches the island in any direction. In anisotropic sticking case with zero sticking probability along Y and unit sticking probability along X direction, the monomer aggregate if it touches the island along the direction of fast diffusion and it retain its identity as monomer if it touches the island along the perpendicular direction.

Results

Figure 1 depicts typical island morphologies for selected D/F ratio, diffusional anisotropy and sticking anisotropy. Figure 2 depicts the variation of island number density N with D/F ratio for different values of DA for the isotropic sticking case. As expected, in high D/F regime, the number density is observed to show power law behaviour $N \sim (D/F)^{-\chi}$ for all diffusional anisotropy case studied. The variation observed is very similar to the results of Mo et al. [5]. We have found that for isotropic sticking case, as DA changes from 1(isotropic diffusion) to $\propto$ (anisotropic diffusion) the exponent is observed to vary from $\chi \sim 0.34 \pm 0.01$ for DA = 1 to 0.28 ± 0.01 for DA = $\propto$. Figure 3 depicts the variation of N with D/F ratio at different values of DA ($1 - \propto$) for perfect anisotropic sticking case. As in the case of isotropic sticking case, here also N decreases with increase in D/F ratio following power law behaviour in high D/F ratio regime. It is seen from figure that in isotropic diffusion case (see curve for DA = 1), the power law behaviour starts to show at relatively low value of D/F ratio. With increase in DA, this starting point is observed to shift to the higher value of D/F ratio as compared to DA = 1 case. In this case, the density exponent is observed to vary from $\chi = 0.31 \pm 0.01$ for isotropic diffusion case to $\chi = 0.24 \pm 0.01$ for anisotropic diffusion case (DA = $\propto$). As a consequence of this behaviour, the influence of DA on number density is observed to depend on D/F ratio. Higher the D/F ratio, the larger the influence in number density by DA is observed. But in the isotropic sticking case, only slight variation in number density with respect to DA is observed.

Figure 4a, b and c depicts the variation of island size distribution Ns(D/F) for three different values of diffusional anisotropy (DA = 1, 10^2 and $\propto$) for isotropic sticking case. As expected, we find that, the D/F ratio influences drastically the island size distribution. As D/F ratio increases, the position of peak of the distribution curve also increase to higher value of s, while, the height of peak decreases. The width of peak also broadens with increase in D/F ratio. In all case of diffusional anisotropy studied, similar change in size distribution are observed (see Fig. 4b, c). In order to observe the effect of DA on size distribution we have plotted size distribution for different DA values for fixed D/F and SA values. Inset to the Fig. 4a depict the variation of size distribution with DA for fixed D/F = $6 * 10^4$ case. A closer look on the figure reveals that the diffusional anisotropy may or may not show its

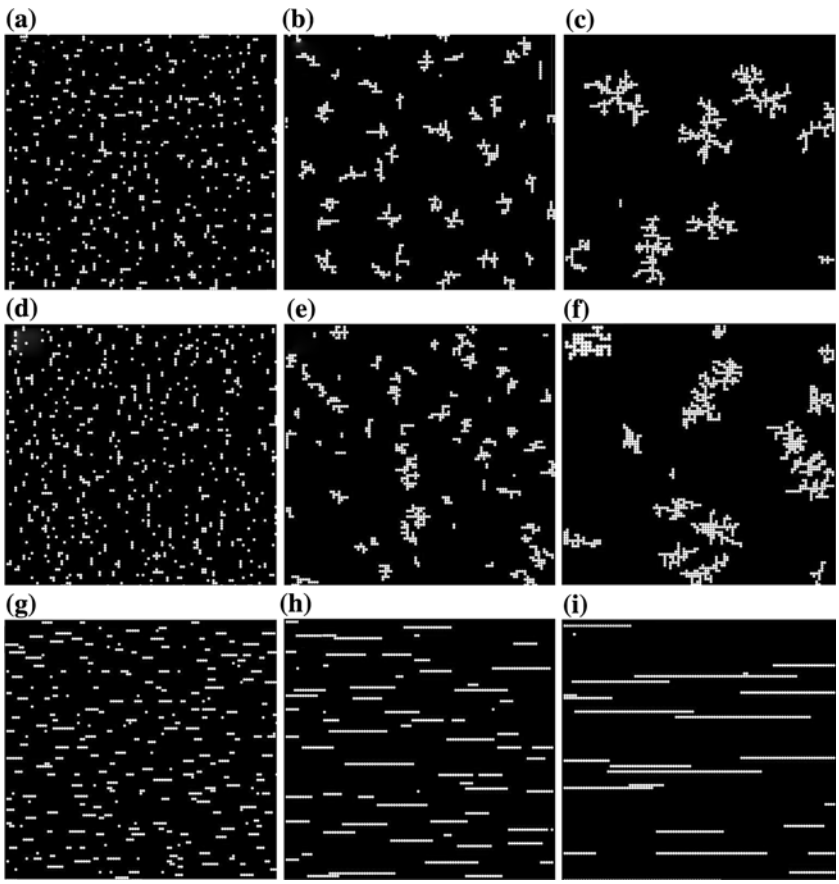

Fig. 1 Picture of typical island morphology for different D/F ratio (600, $6 * 10^5$, and $6 * 10^8$ along horizontal panel) for DA = 1, SA = 1 (**a**, **b** and **c**), DA = $\propto$, SA = 1 (**d**, **e** and **f**) and DA = 1 SA = 0 (**i**, **j** and **k**)

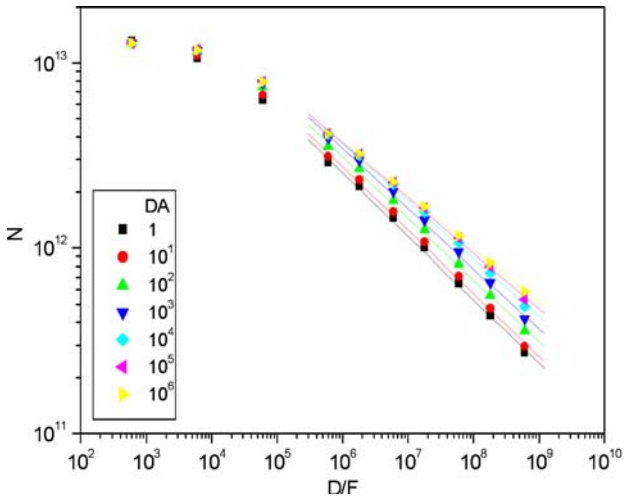

Fig. 2 Log–Log plot showing island density versus D/F ratio for various DA values for isotropic sticking case (SA = 1). The straight line shows the power law fit

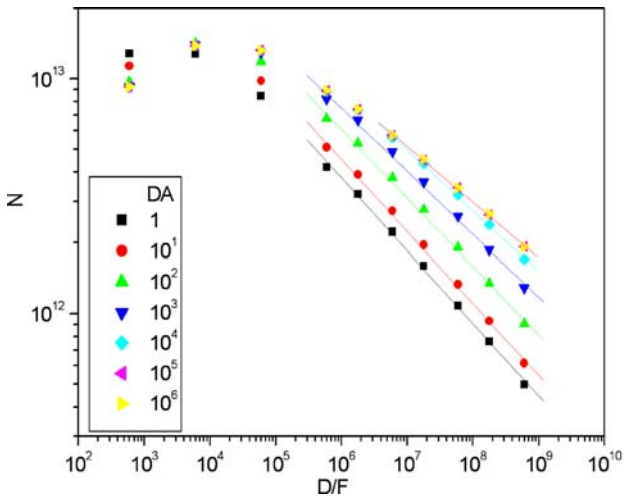

Fig. 3 Log–Log plot showing island density versus D/F ratio for various DA values for anisotropic sticking case (SA = 0). The straight line shows the power law fit

influence depending on its magnitude. As DA increases, the position of peak of the distribution curve is observed to decrease to lower s regime with decrease in its width. Also the peak height is observed to increase with increase in DA value. This is in consistent with the results of number density versus D/F ratio for isotropic sticking case (Fig. 2a), where the total number density is observed to increase with diffusional anisotropy. But if DA is further increased beyond (DA $\geq 10^3$), the size distribution is observed to be unaffected. Similar, behaviour is also observed in other higher D/F ratio cases (see inset to curve Fig. 4b). But in higher D/F ratio case the distribution is observed to unaffected after (DA $\geq 10^3$). Figure 5a, b and c depict the

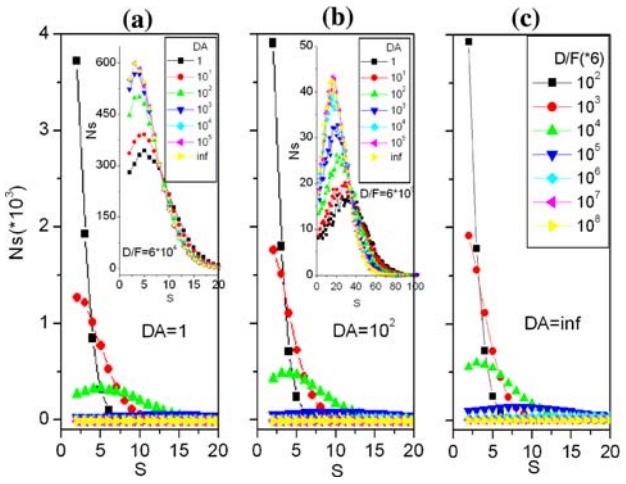

Fig. 4 Island size distribution for 7 different D/F ratio for (**a**) DA = 1 (isotropic diffusion) (**b**) DA = 10^2 and (**c**) DA = ∞ (anisotropic diffusion) for isotropic sticking case. Inset shows size distribution at 7 different DA values for (a) D/F = 6 * 10^4 and (b) D/F = 6 * 10^6

island size distribution Ns (D/F) for three different values of DA (DA = 1, 10^2 and ∞) for anisotropic sticking case. As in the case of isotropic case, the nature of size distribution as well as behaviour of distribution with respect to D/F ratio is almost similar, however the magnitude of Ns differs drastically. Comparing Fig. 5a, b and c for different for different DA values, we have observed that diffusional anisotropy also drastically influence the island size distribution in anisotropic sticking case. As DA value increase, the distribution curve is observed to sharpen. Also the peak of the distribution curve is observed to shift towards the lower island size regime indicating the decrease of the

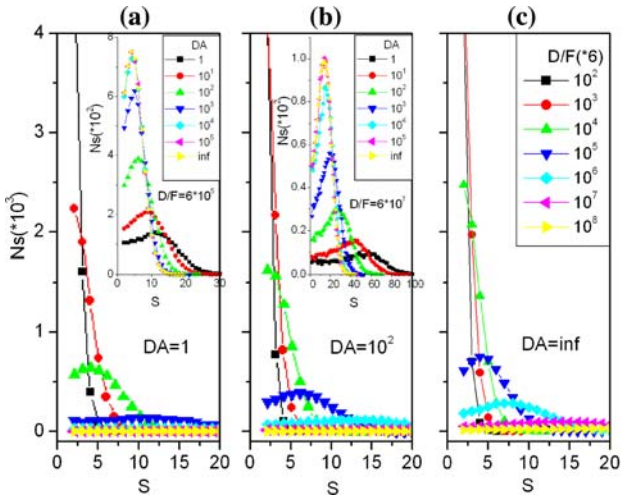

Fig. 5 Island size distribution for 7 different D/F ratio for (**a**) DA = 1 (isotropic diffusion) (**b**) DA = 10^2 and (**c**) DA = ∞ (anisotropic diffusion). Inset shows size distribution at 7 different DA values for (a) D/F = 6 * 10^5 and (b) D/F = 6 * 10^7 for anisotropic sticking case

average island size with DA. The magnitude of Ns also changes drastically with DA. In order to view the influence of DA, we depict the variation of size distribution for different DA value at two fixed D/F ratio ($6 * 10^5$ and $6 * 10^7$) in the inset to the Fig. 5a and b. In anisotropic sticking case also, we found that at high DA value the distribution becomes independent of DA values. Comparing the distribution curve for two different D/F ratio (inset to the Fig 5a and Fig 5b), we find that as D/F ratio increases, the DA value above which the distribution becomes independent also increases. Thus, higher the D/F ratio higher value of DA is needed for island distribution to be independent of diffusional anisotropy. In other words, at a given D/F ratio, higher the difusional anisotropy more the island distribution becomes insensitive to diffusional anisotropy (see inset to Fig. 5a and b).

We have calculated the scaling function f1 defined by equation $f1(S/S_{av}) = Ns(S_{av}*S_{av}/\theta)$ for various diffusional anisotropy case at different sticking anisotropic values. Where S_{av} is the average island size and θ is coverage. In order to observe the influence of diffusional anisotropic on scaling function, we plot the scaling function for different diffusional anisotropy parameter (DA = 1, 10^3, ∞) for two extreme sticking cases. Figure 6a, b and c depict the plot of scaling function f1 for isotropic sticking case for three different DA values (DA = 1, 10^3, ∞). It is seen from the figure that, the island size distributions Ns for different D/F ratio plotted against scaled variable S/S_{av} collapse in a single master curve showing the scaling of the island size distribution. This scaling behaviour is observed in all diffusional anisotropy case showing that the diffusional anisotropy does not alter the scaling of island size distribution. It is also interesting to note that for isotropic sticking case the scaling functions for various diffusional anisotropic parameters are not appreciably different from each other. However, the width of the scaled distribution curve is observed to decrease slightly with increase in DA. The position of peak of the scaled distribution also observed to shift towards the lower value of scaled variable S/S_{av}.

Figure 7 depicts the scaling function for different DA values for anisotropic sticking case. As in isotropic sticking case, we observed that in all diffusional case (DA = $1 - \infty$), the curves for D/F > $6 * 10^4$ collapse into a single master curve. Thus, for anisotropic sticking case also, the island size distribution satisfies the scaling relation given above. Here, in both Figs. 6 and 7, we have also plotted the data for small D/F ratio also. We notice that the quality of data collapse for D/F ratio < $6 * 10^4$) is worse which is shown by line connecting data points. This is because scaling relation holds only for high D/F ratio, which is widely known. Comparing the scaling function at different DA case, we find that as DA increases the height of the peak of scaling function also increase slowly. Further, as in isotropic sticking case, as diffusional anisotropy increases the peak of scaling function shift to the low value of the scaled variable S/S_{av} and the peak for perfect anisotropic diffusion case is slightly sharper than the peak for isotropic diffusion case. Similar results for variation in scaled island distribution for the change in DA = 1 to DA = 10^3 for D/F = 10^9 were observed by Lindroth [15] for model for compact island. However, in their study the diffusional

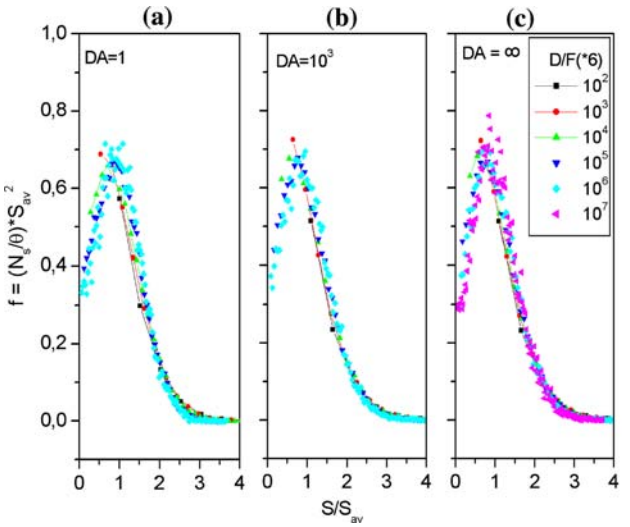

Fig. 6 Plot of scaling function f1 versus the scaled size S/S_{av} for isotropic sticking case for (**a**) DA = 1(isotropic diffusion) (**b**) DA = 10^3 (**c**) DA = ∞(anisotropic diffusion) showing the collapse of island size distributions, for different D/F ratio into single master curve

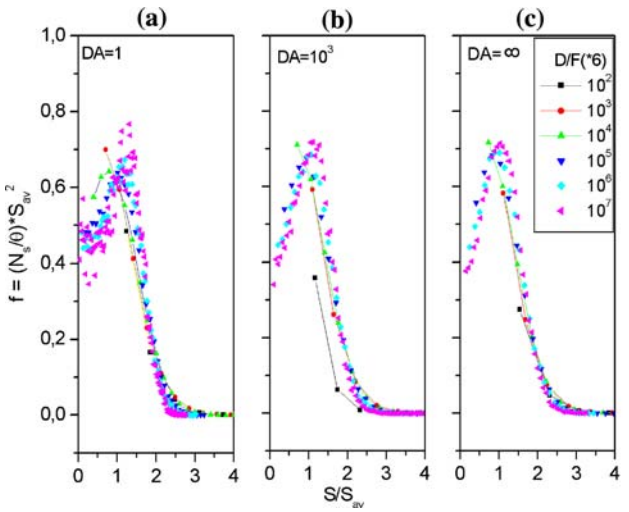

Fig. 7 Plot of scaling function f1 versus the scaled size S/S_{av} for anisotropic sticking case for (**a**) DA = 1(isotropic diffusion) (**b**) DA = 10^3 (**c**) DA = ∞(anisotropic diffusion) showing the collapse of island size distributions, for different D/F ratio into single master curve

anisotropy was observed to produce marked variation in the scaling function.

Discussion

As mentioned earlier, we see that (Figs. 2 and 3), the island density exponent decreases with increase in DA. We can explain this behaviour using probability approach. When the D/F is low, whether motion is 1d or 2d type, the probability of nucleation event will be low. Thus, the island number density does not change appreciably at low D/F. At high D/F, the island density for high DA value is high as compared to the island density for isotropic diffusion. This naturally leads the decrease of exponent with increase in DA. Also in anisotrtopic sticking case, for the same D/F ratio, the probability of adatoms remaining isolated is higher as compared to probability in the isotropic sticking case. This leads to higher nucleation probability and higher number density in anisotropic sticking case for same D/F ratio. Thus, as compared to isotropic sticking case the curve in anisotropic sticking case is shifted upward which is seen in figure (see Figs. 2 and 3). To ease comparison, we have plotted both graphs on the same scale. The shift of curve at high D/F ratio is lesser than shift in low D/F ratio, because at low D/F ratio nucleation probability is high as compared to growth probability where as, at high D/F ratio growth probability is higher than nucleation probability.

We find that, when DA increases distribution function Ns (D/F) is more sharp and peak shift to the left (see inset to Figs. 4 and 5). It is because when diffusion is more anisotropic and when D/F ratio is low, the probability of the adatom to come in contact will be low which leads to more isolated adatoms. In this case, nucleation event dominate the growth event. Thus, at high DA, islands sizes will be small and number will be high. That is, number density of smaller size islands will be higher as compared to the number density of higher sizes islands. But when DA is decreased, the island growth probability will be high and the probability of adatoms remaining as monomer becomes lower. Thus, being lower in monomer density number density the growth probability will be higher resulting island of higher size. Thus, in low diffusional anisotropy case the peak tends to shift towards the high value of S as seen in figure.

We also see that at low D/F ratio, and in high DA range (10^4 – ∞) (see inset to Figs. 4 and 5), the distribution is almost independent of DA value and in low DA value distribution changes drastically. This is because as we know, the higher the diffusional anisotropy lesser will be the probability of adatom to come in contact with island or monomer. Therefore, at sufficiently high anisotropy the probability of adatom to come in contact with monomer or island is very low. This leads island distribution insensitive to DA. But as DA decreases, the probability of finding another adatom or island will increase and this leads to the change in distribution, which is seen in figure.

We also see that in Fig. 7, for the same D/F ratio (D/F = 6 * 10^7), the scaled distribution curve for DA = 1 is much more scattered as compared to the scaled distribution curve for DA = ∞. It is because, at high D/F ratio, the number density of islands for DA = 1 is much lower than the number density for DA = ∞. This lesser in number density cause data scatter more.

Further, in our simulation deposition is stopped after reaching the coverage of 0.07 mL. This coverage is chosen to compare our results with the results with results of Mo et al. (not shown here) in which they have used same coverage in experimental and simulation work to determine diffusion constant and activation energy by measuring the scaling of the island density as a function of temperature [5]. Although, the selected coverage 0.07 mL is slightly low, it is after the onset of the scaling and before the coalescence regime. It is because in coalescence regime island coalescence begins and the island size distribution deviates from the size distribution in the scaling regime, which results in the break down of scaling.

As mentioned above, LaBella et al. [20] had determined the basic diffusion parameters such as activation energy Ea, directional hopping rate (DR) and directional sticking probability ratio (SR) by combined study of STM results and Monte Carlo simulation. They have determined the DR and SR by comparing the STM morphologies with the simulated morphologies. From the simulated results using these diffusion parameters and the temperature dependence of the number density from STM results, activation energy was calculated. As we have seen that the island size distribution is sensitive to both DA as well as SA, we suggest that, the calculation of diffusional parameter and hence the Ea by comparing STM morphology as well as STM size distribution with the simulated one provides the more reliable Ea as compared to the Ea calculated by comparing morphology alone.

Summary and conclusion

We have made systematic study of influence of diffusional anisotropy and sticking anisotropy on island density exponent and island size distribution for lower temperature submonolayer epitaxial growth model using Monte Carlo technique. We have found that for isotropic sticking case, as DA changes from 1 (isotropic diffusion) to infinite (anisotropoic diffusion) the island density exponent is observed to vary from 0.34 ± 0.01 to 0.28 ± 0.01, respectively. In anisotropic sticking case, the density exponent is

observed to vary from $\chi = 0.31 \pm 0.01$ to $\chi = 0.24 \pm 0.01$ for the same variation in diffusional anisotropy. The island size distribution appears to change drastically with diffusional anisotropy in all case sticking anisotropy. However, the magnitude of variation is low as compared to the variation due to D/F ratio. The influence produced by diffusional anisotropy is also observed to depend on D/F ratio. At very low D/F ratio, diffusional anisotropy shows comparatively no influence on size distribution for both sticking condition. In high DA regime also, the size distribution is not influenced by diffusional anisotropy provided D/F ratio is not very high. The scaling behaviour of island size distribution is observed in all diffusional anisotropy case for both isotropic as well as anisotropic sticking case. As diffusional anisotropy increases, the position of peak of the scaled distribution is observed to shift towards the lower value of scaled variable S/S_{av} for both sticking condition.

Acknowledgements One of the authors S.P. Shrestha gratefully acknowledges the support from Swedish International Development Corporation Agency (SIDA) and The Abdus Salam International Center For Theoretical Physics (ICTP) under regular associate scheme.

References

1. Brune H (1998) Surf Sci Rep 31:121
2. Ratsch C, Gyure MM, Chen S, Kang M, Vvedensky DD (2000) Phys Rev B 61:10598
3. Mortensen JJ, Linderoth TR, Jacobsen KW, Laegsgaard E, Stensgaard I, Besenbacher F (1998) Surf Sci 400:290
4. Brune H, Bales GS, Jacobson J, Boragno C, Kern K (1999) Phys Rev B 60:5991
5. Mo YW, Kleiner J, Webb MB, Lagally MG (1991) Phys Rev Lett 66:1998; Mo YW, Kleiner J, Webb MB, Lagally MG (1992) Surf Sci 268: 275
6. Tantaru O, Family F (2000) Phys Rev B 62:13129
7. Stroscio JA, Pierce DT (1994) Phys Rev B 49:8522; Stroscio JA, Pierce DT, Dragoset RA (1993) Phys Rev Lett 70:3615
8. Somfai E, Wolf DE, Kertesz J (1996) J Phys I 6:393
9. Bales GS, Chrzan DC (1994) Phys Rev B 50:6057
10. Lee SB, Gupta BC (2000) Phys Rev B 62:7545; Lee SB (2006) Phys Rev B 73: 035437; Lee SB, Hwangbo T (2004) Physica A 337:470
11. Blackman JA, Mulheran PA (2001) Comp Phys Commun 137:195
12. Smilauer P, Wilby MR, Vvedensky DD (1993) Phys Rev B 47:4119
13. Bartelt MC, Evans JW (1992) Phys Rev B 46:12675; Bartelt MC, Evans JW (1993) Surf Sci 298:421
14. Amar JG, Family F, Lam P (1994) Phys Rev B 50:8781; Amar JG, Family F (1995) Phys Rev Lett 74:2066
15. Linderoth TR, Mortensen JJ, Jacobsen KW, Laegsgaard E, Stensgaard I, Besenbacher F (1996) Phys Rev Lett 77:87
16. Brune H, Roder H, Boragno C, Kern K (1994) Phys Rev Lett 73:1955
17. Muller B, Nedelmann L, Fischer B, Brune H, Kern K (1994) Phys Rev B 54:17858
18. Yang H, Labella VP, Bullock DW, Ding Z, Smathers JB, Thibado PM (1994) J Crystal Growth 201:88
19. Kasu M, Kobayashi N (1994) J Crystal Growth 170:246
20. Labella VP, Bullock DW, Ding Z, Emery C, Harter WG, Thibado PM (2000) J Vac Sci Technol A 18:1526
21. Iguain JL, Martin HO, Aldao CM (1999) Phys Rev B 59:4596
22. Mazzitello KI, Iguain JL, Martin HO (1999) J Phys A: Math Gen 32:4389